Precipitation Doppler Spectrum Reconstruction With Gaussian Process Prior

Dash, T.K.; Driessen, J.N.; Krasnov, O.A.; Yarovoy, Alexander

DOI
10.1109/CAMA57522.2023.10352683

Publication date
2024

Document Version
Final published version

Published in
2023 IEEE Conference on Antenna Measurements and Applications, CAMA 2023

Precipitation Doppler Spectrum Reconstruction with Gaussian Process Prior

Tworit Kumar Dash
Microelectronics
Delft University of Technology
Delft, Netherlands
T.K.Dash@tudelft.nl

Hans Driessen
Microelectronics
TU Delft
Delft, Netherlands
J.N.Driessen@tudelft.nl

Oleg Krasnov
Microelectronics
TU Delft
Delft, Netherlands
O.A.Krasnov@tudelft.nl

Alexander Yarovoy
Microelectronics
TU Delft
Delft, Netherlands
A.Yarovoy@tudelft.nl

2023 IEEE Conference on Antenna Measurements and Applications (CAMA) | 979-8-3503-2304-7/23/$31.00 ©2023 IEEE | DOI: 10.1109/CAMA57522.2023.10352683

***Abstract*—The challenge of reconstructing the Doppler spectrum of a precipitation-like event observed by a fast-scanning weather radar is addressed. A novel method is proposed where the echo sequence in time is assumed to be a complex Gaussian process with a known covariance structure. It is a two-step approach where the first step is the estimation of the hyper-parameters of the covariance function with a maximum likelihood approach, and the second step is the reconstruction of the spectrum directly in the time or spectral domain. The proposed approach is applied to simulated data for hyper-parameter estimation performance analysis and real radar data for the complete Doppler spectrum reconstruction.**

***Index Terms*—Bayesian Inference, Weather Doppler Radar**

I. Introduction

Modern airports deploy fast-scanning phased array radars to detect and track point-like targets such as drones and birds. These radars have phased array architecture in elevation (which allows them to scan the elevation instantaneously electronically) and mechanical scan in azimuth. For point-like targets, a faster update of the complete field of view is necessary, and hence, the radars scan very fast in azimuth. As there is a growing interest in updating these radars for severe weather detection, some new features, such as estimating the intensity of precipitation and retrieving the 3D wind field, need to be added. The abovementioned applications require Doppler processing of the echo samples received from meteorological targets. As the Doppler spectra for such meteorological objects are continuous and extended, the required time on target is usually larger than what is required for point-like targets. Therefore, the fast scanning nature of such radars limits the capability to detect weather targets accurately. The usage of typical weather radars and the traditional techniques to retrieve information from the Doppler spectrum are discussed further.

Doppler weather radars are used primarily to estimate the motion parameters of precipitation-like events with the help of the Doppler spectrum. The motion parameters (also known as the Doppler moments) that are retrieved from the weather radar observations are the total power (zeroth moment), the mean Doppler velocity (first moment), and the Doppler spectrum width (square root of the second central moment). The total power indicates the intensity of the targets in space, the mean Doppler velocity indicates the mean radial velocities of the hydrometeors, and the Doppler spectrum width indicates the velocity dispersion caused by turbulence and other statistical effects (these effects cause broadening of the Doppler spectrum).

Traditional moment estimators require long records of the echo samples to accurately estimate the Doppler moments [1], [2]. However, the moment estimation is often biased due to many factors, such as non-stationarity conditions of the atmosphere and fast radar scans. Furthermore, the traditional non-parametric moment estimators cannot process the echo samples incoherently from multiple radar scans.

Given the short records of the echo samples in time and retrieved moments, the traditional approaches do not attempt to reconstruct the full stochastic Doppler spectrum with local variations across the Doppler frequencies, which could help study the microphysics of such events. The inability of existing weather radar Doppler processing chains to reconstruct the local Doppler spectrum comes from the fact that only the Doppler moments are usually stored for further use rather than the echo samples due to memory limitations.

Due to the abovementioned limitations, a desired signal processing chain should have the following features for fast scanning radars:

1) Accurate estimation of Doppler moments with a short observation period, randomly stored echo samples, and samples collected over multiple scans of a fast scanning radar.
2) Reconstruct the Doppler spectrum local variations with the help of a few echo samples.

In this paper, we propose a novel signal processing pipeline that has several features such as accurate moment estimation with a few echo samples in time, the ability to process the echo samples that are not necessarily coherent (usually

This work was supported by the ‘European Regional Development Fund (ERDF) via the Kansen voor West II program’ under the project ‘Airport Technology Lab’.

realized in a very fast scanning radar with the stationarity assumption of the atmosphere assumed for a short period) and reconstruct the high-resolution local stochastic signal and its spectrum directly using a few echo samples. Therefore, by introducing the proposed processing chain, a few echo samples can be stored from regions of interest in space for later investigations.

II. Traditional Moment Estimators

The traditional Doppler moment estimators for weather radars are categorized into non-parametric and parametric approaches.

A. Non-parametric Moment Estimators

The non-parametric approaches are categorized into Discrete Fourier Transform (DFT) and Auto-Covariance (ACV) based techniques. The performance analysis of the non-parametric methods can be found in [1], [3]–[5]. The DFT-based technique uses the power spectrum of the echo samples to obtain the moments. The ACV-based technique (also called the Pulse Pair estimators or PP) uses ACV with the desired number of sample lags. The different versions of the PP estimator have been studied in [6], [7], [2, Ch. 6, p. 136-138]. The advantage of such non-parametric methods is that they do not consider any specific shape of the Doppler spectrum and are computationally very efficient. The disadvantage of the DFT-based method is that it is usually biased because of the limited observation period. The PP methods are usually less biased for the first moment of Doppler but are biased for the second moment. The different versions of the PP perform better in different intervals of the spectrum widths. To adequately use a suitable PP version, some prior information regarding the range of the spectrum width needs to be known. This paper focuses on fast-scanning radar observations without prior information, so we do not consider the non-parametric approaches.

B. Parametric Moment Estimators

The parametric moment estimators assume a specific structure of the power spectral density (PSD) or the ACV matrix. The PSD-based techniques [8], [9] are usually more accurate than the non-parametric approaches. However, they require a long observation time to estimate the Doppler spectrum width accurately. The ACV-based parametric approaches are the most accurate because they consider all sample lags for the signal and are unaffected by the spectral leakage typically observed in PSD-based techniques. In the signal processing chain proposed in this paper, a parametric moment estimator uses a parametric structure of the ACV matrix.

III. Rationale Behind The Approach, A Bayesian Perspective

As this paper proposes an estimation of the Doppler moments and the reconstruction of the Doppler spectrum with a few echo samples stored in time, a new perspective is put forward. A Bayesian approach has been followed. The complex weather radar echoes are received from an ensemble of many raindrops in a certain volume in space [1], [2, Ch. 4, eq.(4.1), p. 67], the sequence of echo samples can be considered a complex Gaussian process (CGP) with zero mean, covariance function C and pseudo-covariance P. The PSD of the same process can be determined by taking the Fourier transform (FT) of the covariance. We consider the stationarity condition of the rainy events for a short period; therefore, we can assume that the covariance is a function of only the time difference between the echo samples and not the absolute time instances $C(t_p, t_q) = C(t_p - t_q)$. We consider a parametric form of the covariance function with parameters denoted as Θ. From a Bayesian perspective, the model is assumed for the time domain sequence itself (as a CGP); the parameters of its covariance are usually referred to as hyper-parameters. The CGP of the echo samples in time can be expressed as the following [10].

$$z(t) \sim \mathcal{CGP}(0, C(\Theta), P(\Theta)) \tag{1}$$

The covariance and pseudo-covariance are given as:

$$C(t_p, t_q) = \mathbb{E}[z(t_p) z^*(t_q)] \tag{2}$$

$$P(t_p, t_q) = \mathbb{E}[z(t_p) z(t_q)] \tag{3}$$

In some special cases, such as typical weather radar echoes, the Gaussian process is circularly symmetric, meaning that the pseudo-covariance is 0. The complex covariance function can be written as:

$$\mathbf{C} = \mathbf{C_{rr}} + \mathbf{C_{ii}} + \mathbf{j}(\mathbf{C_{ir}} - \mathbf{C_{ri}}), \tag{4}$$

where $\mathbf{C_{rr}}$, and $\mathbf{C_{ii}}$ are the covariances of the real and imaginary parts only. The covariances $\mathbf{C_{ri}}$, and $\mathbf{C_{ir}}$ are the cross-covariances of the real and imaginary parts, and $j = \sqrt{-1}$. For a proper complex Gaussian process, the following identities hold:

$$\mathbf{C_{rr}} = \mathbf{C_{ii}} \tag{5}$$

$$\mathbf{C_{ir}} = \mathbf{C_{ri}}^T = -\mathbf{C_{ri}} \tag{6}$$

The complex covariance function can be expressed in a matrix form with only real entries as follows:

$$\mathbf{C_R} = \begin{bmatrix} \mathbf{C_{rr}} & \mathbf{C_{ri}} \\ -\mathbf{C_{ri}} & \mathbf{C_{ii}} \end{bmatrix} \tag{7}$$

This real valued covariance matrix formulation of (7) is advantageous when dealing with complex valued observations. The complex valued observations can be stacked-up as one column vector with real and imaginary parts.

$$\mathbf{z_{r,i}} = \begin{bmatrix} \Re(\mathbf{z^T}), & \Im(\mathbf{z^T}) \end{bmatrix}^{\mathbf{T}} \tag{8}$$

Gaussian process regression has two steps. Firstly, the hyper-parameters are estimated by maximizing the marginal log-likelihood. The second step is sampling from a posterior distribution. These steps are explained in detail in the following sub-sections.

A. Hyper-parameter Estimation (Training the CGP)

Modeling the signal sequence as a circular CGP gives us the advantage of using the well-defined marginal log-likelihood to estimate the hyper-parameters Θ. The log-likelihood is given by (derived from the probability density function of [10, eq. (13)]:

$$\log(p(\mathbf{z}|\Theta)) = -\mathbf{z}^H(\mathbf{C}+\sigma_{\mathbf{n}}^{\mathbf{2}}\mathbf{I_N})^{-1}\mathbf{z} \quad (9)$$
$$-\log|\mathbf{C}+\sigma_n^2\mathbf{I_N}| - N\log(\pi), \quad (10)$$

where ^{H} is the Hermitian operator, $||$ is the determinant operator, and $\sigma_n^2\mathbf{I_N}$ is the covariance matrix of a zero mean white Gaussian noise (N is the number of data points). The hyper-parameters can be estimated by maximum likelihood estimation. It is worth noting that in (9) the covariance matrix used is the complex one (4) and the observations are also directly the complex observations $\mathbf{z}$.

$$\hat{\Theta} = \max_{\Theta}\log(p(z|\Theta)). \quad (11)$$

B. Posterior in Time Domain

After obtaining the estimates of the Doppler moments, the posterior can be obtained both in time and frequency domains directly using the time domain observations. The posterior outputs are jointly proper with the training data (observed data). The mean and covariance of the posterior outputs are given below.

$$\hat{\mathbf{m}}_{\mathbf{r,i}}(\mathbf{t}^*) = \mathbf{C}^{\mathbf{T}}(\mathbf{t},\mathbf{t}^*)\mathbf{C_{CN}}^{-\mathbf{1}}(\mathbf{t},\mathbf{t})\mathbf{z}_{\mathbf{r,i}}, \quad (12)$$

$$\hat{\mathbf{C}}(\mathbf{t}^*,\mathbf{t}^*) = \mathbf{C}(\mathbf{t}^*,\mathbf{t}^*) - \mathbf{C}(\mathbf{t},\mathbf{t}^*)^{\mathbf{T}}\mathbf{C_{CN}}^{-\mathbf{1}}(\mathbf{t},\mathbf{t})\,\mathbf{C}(\mathbf{t},\mathbf{t}^*), \quad (13)$$

where $\mathbf{t}$ are the time instances of the observations and $\mathbf{t}^*$ are the desired time instances for the posterior. The observations $\mathbf{z}$ have the same dimension as $\mathbf{t}$. The lower case letters in bold represent vectors, whereas the bold upper case letters represent matrices. The $\hat{}$ superscript refers to an estimated/ posterior quantity. The covariance with the subscript $_{\mathrm{CN}}$ refers to the covariance of the data with added covariance of a white Gaussian noise sequence.

$$\mathbf{C_{CN}} = \mathbf{C_R} + \sigma^{\mathbf{2}}{}_{\mathbf{n}}\mathbf{I_{2N}} \quad (14)$$

C. Posterior in Frequency Domain

The frequency domain posterior can be sampled directly from a Gaussian process having the following mean and covariance [11] (because the time domain signal and the spectrum functions are jointly proper):

$$\hat{\mathbf{m}}^*_{\mathbf{F(r,i)}} = \mathbf{C_{tF}}(\mathbf{t},\mathbf{f})^{\mathbf{T}}\mathbf{C_{CN}}^{-\mathbf{1}}(\mathbf{t},\mathbf{t})\mathbf{z}_{\mathbf{r,i}} \quad (15)$$

$$\hat{\mathbf{C}}(\mathbf{f},\mathbf{f}) = \mathbf{C_{FF}}(\mathbf{f},\mathbf{f}) - \mathbf{C_{tF}}(\mathbf{t},\mathbf{f})^{\mathbf{T}}\mathbf{C_{CN}}^{-\mathbf{1}}(\mathbf{t},\mathbf{t})\,\mathbf{C_{tF}}(\mathbf{t},\mathbf{f}), \quad (16)$$

where $\mathbf{f}$ are the desired frequency points where the posterior needs to be sampled. In (15) and (16), there are two extra covariance matrices used along with $\mathbf{C_{CN}}$. The covariance matrix $\mathbf{C_{FF}}$ is nothing but the covariance of the local spectrum $C_F(f)$ [11] and is the FT of the covariance matrix in the time domain $\mathbf{C}$.

$$\mathbf{C_{FF}} = \begin{pmatrix} \mathbf{C_{Frr}} & \mathbf{0} \\ \mathbf{0} & \mathbf{C_{Frr}} \end{pmatrix} \quad (17)$$

The entries of the $\mathbf{C_{Frr}}$ are given by:

$$C_{Frr}(f_p, f_q) = \frac{1}{2}FT(C(\tau))(\rho)\Big|_{\rho=\frac{f_p+f_q}{2}} \quad (18)$$

The cross-dagonal terms are 0 because the Fourier transform of the time covariance is a real-valued function. The formulation of this covariance matrix is the same as given in [11] but without consideration of the window function. The cross-covariance between the local spectrum and the time series can be expressed as:

$$\mathbf{C_{tF}} = \begin{pmatrix} \mathbf{C_{tFrr}} & \mathbf{C_{tFri}} \\ -\mathbf{C_{tFri}} & \mathbf{C_{tFrr}} \end{pmatrix} \quad (19)$$

The entries of $\mathbf{C_{tFrr}}$, and $\mathbf{C_{tFri}}$ are:

$$C_{tFrr}(t,f) = FT(C(\tau))(f)\cos(2\pi f t) \quad (20)$$

$$C_{tFri}(t,f) = -FT(C(\tau))(f)\sin(2\pi f t) \quad (21)$$

The covariance functions of typical weather like Doppler time sequences are explained in the following section.

IV. Covariance Models For Weather Echoes

The signal model with the Doppler moments as parameters are referred from [1]. Using the same signal model, and by using (2), it can be shown that the covariance function has the following expression:

$$\begin{aligned} C_{CN}(t_p,t_q) = {} & R\exp\left(-8\pi^2T^2\sigma_v^2(t_p-t_q)^2/\lambda\right) \\ & \times\exp\left(j\frac{4\pi T}{\lambda}\mu_v(t_p-t_q)\right) \\ & +\sigma_n^2\delta(t_p-t_q), \end{aligned} \quad (22)$$

where v is the radial velocity, R is the total power of the signal PSD, μ_v and σ_v are the mean Doppler velocity and the Doppler spectrum width, λ is the central wavelength, T is the pulse repetition time of the radar. For simplicity, we use normalized frequency quantities (normalized with the maximum unambiguous frequency) instead of velocities for the parameters and denote the normalized parameters with a subscript $_n$. Therefore, using $\mu_{fn} = 2\mu_v T/\lambda$, and $\sigma_{fn} = 2\sigma_v T/\lambda$, the covariance can be rewritten as:

$$\begin{aligned} C_{CN}(t_p,t_q) = {} & R\exp\left(-2\pi^2\sigma_{fn}^2(t_p-t_q)^2\right) \\ & \times\exp\left(j2\pi\mu_{fn}(t_p-t_q)\right) \\ & +\sigma_n^2\delta(t_p-t_q). \end{aligned} \quad (23)$$

The model of the $\mathbf{C_{Frr}}$ therefore can be given by the FT of the covariance function.

$$C_{Frr}(f) = \frac{R}{2\sqrt{2\pi\sigma_{fn}^2}} \exp\left(-\frac{(\mu_{fn}-f)^2}{2\sigma_{fn}^2}\right) \tag{24}$$

The covariance $\mathbf{C_{tF}}$ can therefore be expressed in closed forms based on 20, and 21. In practice, for radar applications, obtaining an estimate of noise variance is possible experimentally. Moreover, in estimation problems, the power/ amplitude is often considered a nuisance parameter. An estimate of R can be obtained by taking the average power of the signal in time domain. Therefore, in this paper, we assume that the power R and the noise variance σ_n^2 are known quantities.

V. Performance of Hyper-parameter Estimation

The signal model of [1] is used to simulate the weather echoes in time with various normalized spectrum widths and a fixed normalized mean Doppler $\mu_{fn} = 0$ (the number of echo samples $N = 32$). The samples in time are coherent to make a fair comparison with the non-parametric techniques. A Monte-Carlo simulation is performed for each spectral width at a fixed noise level with 12 dB input SNR [12]. The hyper-parameters (Doppler moments) are computed by maximizing the log-likelihood (9). The optimization is performed using the active-set and the Limited Memory Broyden–Fletcher–Goldfarb–Shanno (L-BFGS) algorithms [13]. This method is preferred for its shorter computation time. The bias and standard deviation of both moment estimates with 1024 Monte-Carlo runs are shown in Fig. 1 with two other non-parametric techniques (DFT and PP). It can be observed that the bias and standard deviations obtained by the proposed approach (GP) are better than DFT and PP for ($\sigma_{fn} < 0.2$). However, especially for very high spectrum widths ($\sigma_{fn} > 0.2$), PP has a lower bias. The DFT approach has lower standard deviation for ($\sigma_{fn} > 0.2$) than other approaches due to its considerable bias.

VI. Application to Real Radar Data

The Doppler spectrum reconstruction is performed with data collected from a rain event on May 9, 2023 from the X-band FMCW MESEWI radar (from the horizontal polarization “HH” channel) at the Delft University of Technology, Netherlands. The radar parameters are shown in Table I. The sampled intermediate frequency data is processed as follows. After DC compensation, range processing is carried out by a FFT in fast time domain. The mean is subtracted from each slow time sequence to remove the effect of the clutter. The Doppler processing is carried out in each range-azimuth cell. However, in this paper, we show the reconstruction of the Doppler spectrum at one resolution cell that had a range of 1.27 km from the radar and at an azimuth of 277° in a clockwise direction from the geographical north. The elevation at which this data was acquired was 30°.

The radar scan speed was one rotation per minute 1 rpm. We have 512 echo samples from each resolution cell for Doppler processing. To simulate a condition where only a few

TABLE I
MESEWI Radar Parameters

Parameter	Value
Center Frequency (f_c) (Hz)	9.4×10^9
Bandwidth (BW) (Hz)	50×10^6
PRI (T)	$813.2\mu s$
Beamwidth in Azimuth ($d\phi$)	$2.5°$
Elevation Angle (ψ)	$30°$
ADC Sampling f_s (Hz)	4.92×10^6

samples are available, we randomly choose samples from this sequence as measurements to be used for the reconstruction. However, the proposed approach can also be used when only a few samples from a very fast scanning radar (from a single or several scans) are used (considering the stationarity condition of the atmosphere for a short period). We choose a few random samples for this research to show that the proposed approach can reconstruct the Doppler spectrum of extended weather targets with only a few incoherent measurements.

The posterior mean, several realizations of the posterior with two standard deviation bounds for the time domain signal, is shown in Fig. 2. In the figures, “GT” stands for the ground truth, which incorporates all the 512 samples in the sequence. Of these measurements, only a few (less than 7%) are used for the reconstruction.

The mean posterior of the power spectrum is shown along with the ground truth power spectrum and the DFT power spectrum of only the available samples in Fig. 3.

In the time domain reconstruction, it can be observed that the mean posterior converges to the available observations. The mean posterior has a similar trend to the ground truth sequence. Similarly, In the frequency domain reconstructions, including the power spectrum, the mean posterior has a similar trend as the ground truth spectrum. The posterior two standard deviation bounds adequately capture the signal in both the time and frequency domain. A performance metric for the quality of the posterior reconstruction with SNR, the spectral width, and the number of available measurements should be developed further(which is not considered in this paper).

VII. Conclusions

A novel two-step approach has been proposed in this paper for Doppler spectrum reconstruction for precipitation-like extended targets. The proposed approach is based on the principles of complex Gaussian processes. The first step in the two-step approach is to estimate the hyper-parameters of the covariance function of the complex Gaussian process. The analogy of the hyper-parameter estimation of a Gaussian process with traditional Doppler moments estimation is justified. The performance analysis of the hyper-parameter estimation is presented, and it is shown that the bias and variance of the proposed approach are lower than the existing non-parametric Doppler moment estimators (DFT and PP) for a broad range of Doppler spectrum widths. The second step is reconstructing the signal and the signal spectrum with the

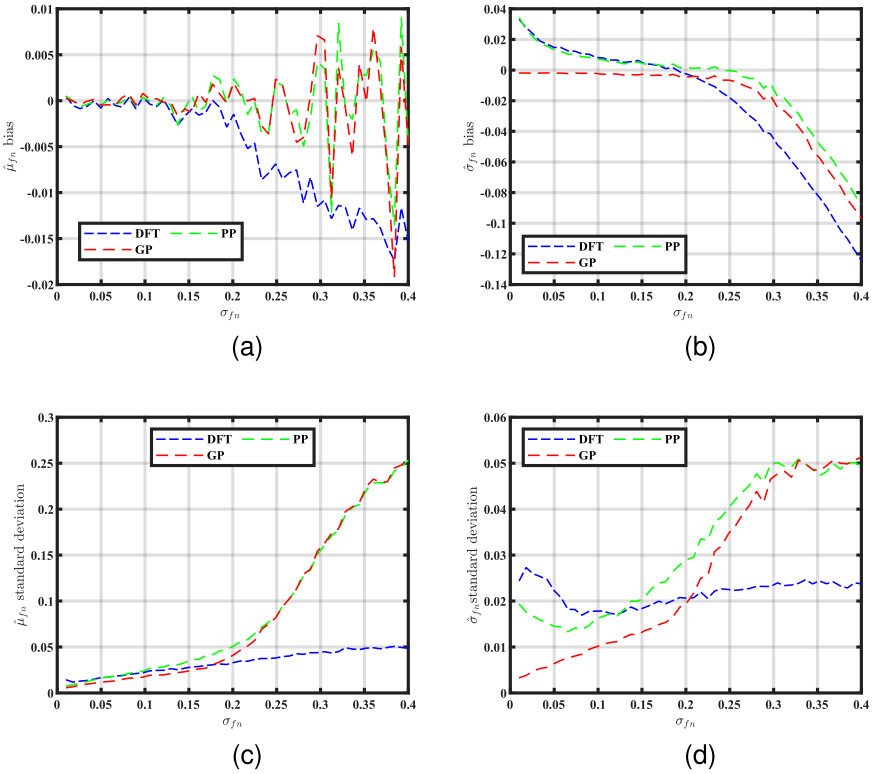

Fig. 1. Performance of the hyper-parameter estimation for with respect to σ_{fn} at $\mu_{fn} = 0$. (a) Biases in the estimates of the Mean Doppler Frequency normalized $\hat{\mu}_{fn}$, (b) Doppler frequency width normalized $\hat{\sigma}_{fn}$. (c) Standard deviation of the estimates of the Mean Doppler Frequency normalized $\hat{\mu}_{fn}$, (d) the Doppler Spectrum Width normalized $\hat{\sigma}_{fn}$.

help of only a few observations in time. A typical application of such a scenario is realized in the case of fast scanning weather radars where the the total observation time is very low. As Gaussian process regression is a Bayesian approach, it accounts for its uncertainty. Therefore, instead of only a unique reconstruction, it provides several different realizations of the reconstruction. The Doppler spectrum reconstruction is applied to the real radar data obtained from the MESEWI radar at Delft University. A large record of echo samples was stored, and a few of those (less than 7%) were used for the reconstruction, and the reconstruction was compared with the original signal. It is shown that the reconstruction of the signal and the spectrum have the same trends as the original one.

Although a circularly symmetric covariance function assumption for the weather echoes is appropriate, more investigation is needed for different types of weather conditions. Furthermore, more studies should be performed to develop appropriate metrics to assess the performance of the posterior estimates of the signal and the spectrum for both stationary and non-stationary weather echoes.

Acknowledgment

This research was funded by the 'European Regional Development Fund (ERDF) via the Kansen voor West II program' under the project 'Airport Technology Lab'. The authors thank ing. F. van der Zwan for his support during the experiments.

References

[1] T. Dash, O. A. Krasnov, and A. G. Yarovoy, "Performance Analysis of the Wind Field Estimation for a Very Fast Scanning Weather Radar," *Proceedings International Radar Symposium*, vol. 2022-Septe, pp. 420–425, 2022.

[2] R. Doviak and D. Zrnić, *Doppler Radar and Weather Observations*, 2nd ed., 1993.

[3] D. Sirmans and B. Bumgarner, "Numerical Comparison of Five Mean Frequency Estimators," *Journal of Applied Meteorology*, vol. 14, no. 6, pp. 991–1003, 9 1975.

[4] P. R. Mahapatra and D. S. Zrnić, "Practical Algorithms for Mean Velocity Estimation in Pulse Doppler Weather Radars Using a Small Number of Samples," *IEEE Transactions on Geoscience and Remote Sensing*, vol. GE-21, no. 4, pp. 491–501, 1983.

[5] D. S. Zrnic, "Spectral Moment Estimates from Correlated Pulse Pairs," *IEEE Transactions on Aerospace and Electronic Systems*, vol. AES-13, no. 4, pp. 344–354, 1977.

[6] D. Warde, D. Schvartzman, and C. D. Curtis, "Generalized Multi-Lag Estimators (GMLE) for Polarimetric Weather Radar Observations," *IEEE Transactions on Geoscience and Remote Sensing*, vol. 61, pp. 1–12, 2023.

[7] G. Meymaris, J. K. Williams, and J. C. Hubbert, "Performance of a Proposed Hybrid Spectrum Width Estimator for the NEXRAD ORDA," *25th Conference on International Interactive Information and Processing Systems for Meteorology, Oceanography and Hydrology*, pp. 1–9, 2009.

[8] M. J. Levin, "Power Spectrum Parameter Estimation," *IEEE Transactions on Information Theory*, vol. 11, no. 1, pp. 100–107, 1965.

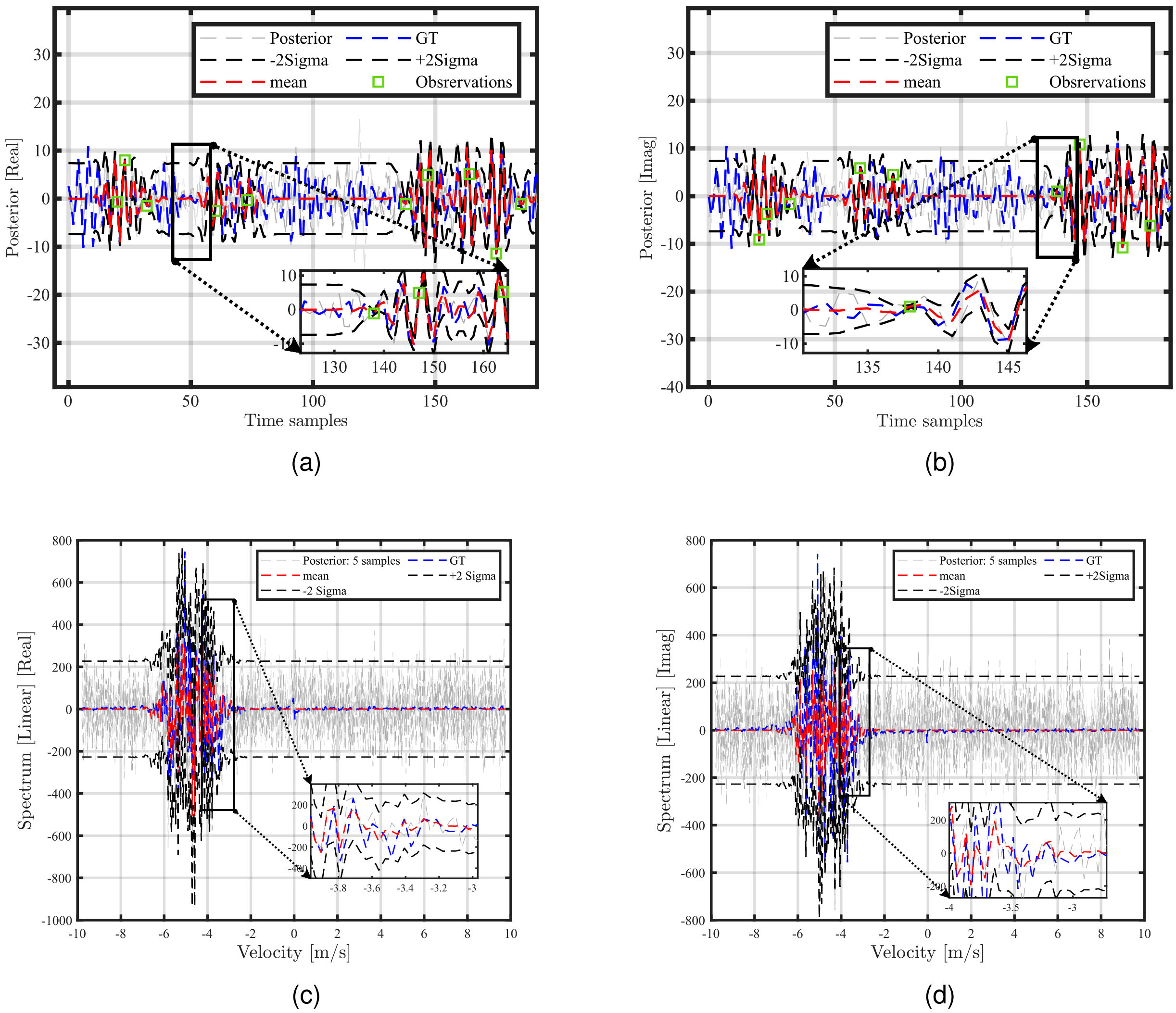

Fig. 2. Reconstruction in time and frequency domain (a) Real part of the time domain signal (b) Imaginary part of the signal in time domain (c) Real part of the local spectrum. (d) Imaginary part of the local spectrum.

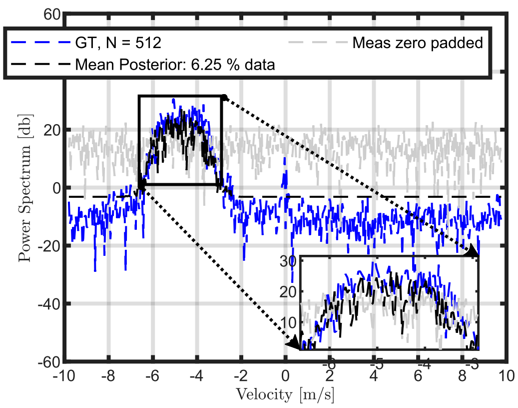

Fig. 3. Power Spectrum Reconstruction

[9] J. M. Dias and J. M. Leitão, "Maximum likelihood estimation of spectral moments at low signal to noise ratios," *ICASSP, IEEE International Conference on Acoustics, Speech and Signal Processing - Proceedings*, vol. 4, pp. 149–152, 1993.

[10] R. Boloix-Tortosa, J. J. Murillo-Fuentes, F. J. Payan-Somet, and F. Perez-Cruz, "Complex Gaussian Processes for Regression," *IEEE Transactions on Neural Networks and Learning Systems*, vol. 29, no. 11, pp. 5499–5511, 2018.

[11] F. Tobar, "Bayesian nonparametric spectral estimation," *Advances in Neural Information Processing Systems*, vol. 2018-Decem, no. NeurIPS, pp. 10 127–10 137, 2018.

[12] D. S. Zrnić, "Simulation of Weatherlike Doppler Spectra and Signals," *Journal of Applied Meteorology*, vol. 14, no. 4, pp. 619–620, 6 1975.

[13] T. Liu and D. Li, "Convergence of the BFGS-SQP method for degenerate problems," *Numerical Functional Analysis and Optimization*, vol. 28, no. 7-8, pp. 927–944, 2007.